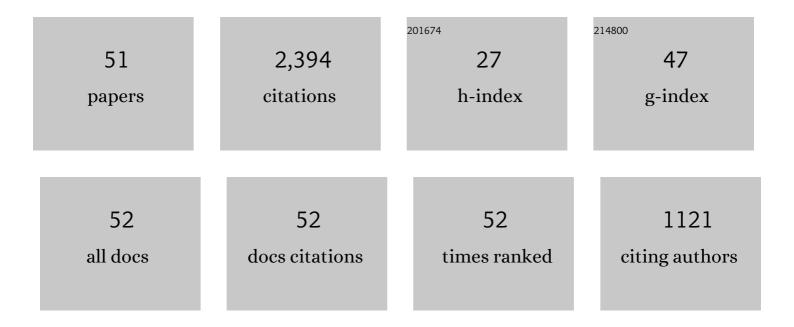
Jienan Pan

List of Publications by Year in descending order

Source: https://exaly.com/author-pdf/1434631/publications.pdf Version: 2024-02-01



Ιτένιανι Ράνι

| # | Article | IF | CITATIONS |
|----|---|-----|-----------|
| 1 | The impact of tectonic stress chemistry on mineralization processes: A review. Solid Earth Sciences, 2022, 7, 151-166. | 1.7 | 2 |
| 2 | Using Raman spectroscopy to evaluate coal maturity: The problem. Fuel, 2022, 312, 122811. | 6.4 | 9 |
| 3 | Fracture variation in high-rank coal induced by hydraulic fracturing using X-ray computer tomography and digital volume correlation. International Journal of Coal Geology, 2022, 252, 103942. | 5.0 | 38 |
| 4 | Simulation of Gas Production Mechanisms in Shear Deformation of Medium-Rank Coal. ACS Omega, 2022, 7, 342-350. | 3.5 | 3 |
| 5 | Micro-nano-scale pore stimulation of coalbed methane reservoirs caused by hydraulic fracturing experiments. Journal of Petroleum Science and Engineering, 2022, 214, 110512. | 4.2 | 18 |
| 6 | Characteristics of Coal Porosity Changes before and after Triaxial Compression Shear Deformation under Different Confining Pressures. ACS Omega, 2022, 7, 16728-16739. | 3.5 | 3 |
| 7 | Similar Material Proportioning and Preparation of Ductile Surrounding Rocks for Simulating In Situ Coalbed methane Production from Tectonically Deformed Coals. Rock Mechanics and Rock Engineering, 2022, 55, 5377-5392. | 5.4 | 4 |
| 8 | Organic-rich siliceous rocks in the upper Permian Dalong Formation (NW middle Yangtze): Provenance, paleoclimate and paleoenvironment. Marine and Petroleum Geology, 2021, 123, 104728. | 3.3 | 30 |
| 9 | Effect of Temperature and Pressure on Nanoscale Pores in Closed Coal. Journal of Nanoscience and Nanotechnology, 2021, 21, 567-577. | 0.9 | 0 |
| 10 | Research on Molecular Structure Characteristics of Vitrinite and Inertinite from Bituminous Coal with FTIR, Micro-Raman, and XRD Spectroscopy. Energy & Fuels, 2021, 35, 1322-1335. | 5.1 | 34 |
| 11 | Network fracturing technology of hydraulic fracturing in coalbed methane reservoir based on induced stress. Arabian Journal of Geosciences, 2021, 14, 1. | 1.3 | 3 |
| 12 | Influences of hydraulic fracturing on microfractures of high-rank coal under different in-situ stress conditions. Fuel, 2021, 287, 119566. | 6.4 | 68 |
| 13 | Macromolecular Structure Changes of Tectonically Deformed Coal: Evidence from Coal Pyrolysis, ¹³ C NMR, and XRD Experiments. Energy & Fuels, 2021, 35, 8711-8722. | 5.1 | 5 |
| 14 | Coal Pores: Methods, Types, and Characteristics. Energy & amp; Fuels, 2021, 35, 7467-7484. | 5.1 | 50 |
| 15 | Organic matter provenance and accumulation of transitional facies coal and mudstone in Yangquan, China: Insights from petrology and geochemistry. Journal of Natural Gas Science and Engineering, 2021, 94, 104076. | 4.4 | 15 |
| 16 | Stress degradation mechanism of coal macromolecular structure: Insights from molecular dynamics simulation and quantum chemistry calculations. Fuel, 2021, 303, 121258. | 6.4 | 18 |
| 17 | Influence of In Situ Stress on Well Test Permeability and Hydraulic Fracturing of the Fanzhuang Block, Qinshui Basin. Energy & Fuels, 2021, 35, 2121-2133. | 5.1 | 13 |
| 18 | Effect of the Coal Molecular Structure on the Micropore Volume and the Coalbed Methane Content. Energy & Fuels, 2021, 35, 19437-19447. | 5.1 | 11 |

Jienan Pan

| # | Article | IF | CITATIONS |
|----|---|------|-----------|
| 19 | Macromolecular structural response of Wender coal under tensile stress via molecular dynamics. Fuel, 2020, 265, 116938. | 6.4 | 16 |
| 20 | 3D microfracture network and seepage characteristics of low-volatility bituminous coal based on nano-CT. Journal of Natural Gas Science and Engineering, 2020, 83, 103556. | 4.4 | 31 |
| 21 | Characterization of coal-based humic acids in relation to their preparation methods. Energy Sources, Part A: Recovery, Utilization and Environmental Effects, 2020, , 1-11. | 2.3 | 2 |
| 22 | Heterogeneity of pore structure of late Paleozoic transitional facies coal-bearing shale in the Southern North China and its main controlling factors. Marine and Petroleum Geology, 2020, 122, 104710. | 3.3 | 23 |
| 23 | Characterizing the shape, size, and distribution heterogeneity of pore-fractures in high rank coal based on X-ray CT image analysis and mercury intrusion porosimetry. Fuel, 2020, 282, 118754. | 6.4 | 48 |
| 24 | Numerical Simulation of Matrix Swelling and Its Effects on Fracture Structure and Permeability for a High-Rank Coal Based on X-ray Micro-CT Image Processing Techniques. Energy & Fuels, 2020, 34, 10801-10809. | 5.1 | 11 |
| 25 | Characterization of Ultramicropores and Analysis of Their Evolution in Tectonically Deformed Coals by Low-Pressure CO ₂ Adsorption, XRD, and HRTEM Techniques. Energy & Fuels, 2020, 34, 9436-9449. | 5.1 | 12 |
| 26 | Potential impact of CO2 injection into coal matrix in molecular terms. Chemical Engineering Journal, 2020, 401, 126071. | 12.7 | 46 |
| 27 | CO2 adsorption and swelling of coal under constrained conditions and their stage-change relationship. Journal of Natural Gas Science and Engineering, 2020, 76, 103205. | 4.4 | 33 |
| 28 | The fracture anisotropic evolution of different ranking coals in Shanxi Province, China. Journal of Petroleum Science and Engineering, 2019, 182, 106281. | 4.2 | 10 |
| 29 | Characteristics of multi-scale pore structure of coal and its influence on permeability. Natural Gas Industry B, 2019, 6, 357-365. | 3.4 | 31 |
| 30 | Fractal study of adsorption-pores in pulverized coals with various metamorphism degrees using N2 adsorption, X-ray scattering and image analysis methods. Journal of Petroleum Science and Engineering, 2019, 176, 584-593. | 4.2 | 59 |
| 31 | Coal microcrystalline structural changes related to methane adsorption/desorption. Fuel, 2019, 239, 13-23. | 6.4 | 77 |
| 32 | Micrometer-scale fractures in coal related to coal rank based on micro-CT scanning and fractal theory. Fuel, 2018, 212, 162-172. | 6.4 | 140 |
| 33 | Anisotropic characteristics of low-rank coal fractures in the Fukang mining area, China. Fuel, 2018, 211, 182-193. | 6.4 | 110 |
| 34 | Changes in the anisotropic permeability of low-rank coal under varying effective stress in Fukang mining area, China. Fuel, 2018, 234, 1481-1497. | 6.4 | 74 |
| 35 | Effects of Metamorphism and Deformation on the Coal Macromolecular Structure by Laser Raman Spectroscopy. Energy & Fuels, 2017, 31, 1136-1146. | 5.1 | 74 |
| 36 | The evolution and formation mechanisms of closed pores in coal. Fuel, 2017, 200, 555-563. | 6.4 | 76 |

Jienan Pan

| # | Article | IF | CITATIONS |
|----|--|-----|-----------|
| 37 | The impacts of stress on the chemical structure of coals: a mini-review based on the recent development of mechanochemistry. Science Bulletin, 2017, 62, 965-970. | 9.0 | 47 |
| 38 | Pore structure characteristics of coal-bearing organic shale in Yuzhou coalfield, China using low pressure N 2 adsorption and FESEM methods. Journal of Petroleum Science and Engineering, 2017, 153, 234-243. | 4.2 | 58 |
| 39 | The Super-Micropores in Macromolecular Structure of Tectonically Deformed Coal Using High-Resolution Transmission Electron Microscopy. Journal of Nanoscience and Nanotechnology, 2017, 17, 6982-6990. | 0.9 | 8 |
| 40 | The role of structure defects in the deformation of anthracite and their influence on the macromolecular structure. Fuel, 2017, 206, 1-9. | 6.4 | 55 |
| 41 | Micro-pores and fractures of coals analysed by field emission scanning electron microscopy and fractal theory. Fuel, 2016, 164, 277-285. | 6.4 | 118 |
| 42 | The closed pores of tectonically deformed coal studied by small-angle X-ray scattering and liquid nitrogen adsorption. Microporous and Mesoporous Materials, 2016, 224, 245-252. | 4.4 | 120 |
| 43 | Quantitative study of the macromolecular structures of tectonically deformed coal using high-resolution transmission electron microscopy. Journal of Natural Gas Science and Engineering, 2015, 27, 1852-1862. | 4.4 | 65 |
| 44 | Nanoscale Pores in Coal Related to Coal Rank and Deformation Structures. Transport in Porous Media, 2015, 107, 543-554. | 2.6 | 82 |
| 45 | Relationship between macro-fracture density, P-wave velocity, and permeability of coal. Journal of Applied Geophysics, 2015, 117, 111-117. | 2.1 | 54 |
| 46 | Examination of the formation phases of coalbed methane reservoirs in the Lu'an mining area (China) based on a fluid inclusion analysis and Ro method. Journal of Natural Gas Science and Engineering, 2015, 22, 73-82. | 4.4 | 13 |
| 47 | Macromolecular and pore structures of Chinese tectonically deformed coal studied by atomic force microscopy. Fuel, 2015, 139, 94-101. | 6.4 | 211 |
| 48 | Coalbed methane sorption related to coal deformation structures at different temperatures and pressures. Fuel, 2012, 102, 760-765. | 6.4 | 187 |
| 49 | Comparison of coalbed gas generation between Huaibei-Huainan coalfields and Qinshui coal basin based on the tectono-thermal modeling. Science China Earth Sciences, 2011, 54, 1069-1077. | 5.2 | 28 |
| 50 | The characteristics and origins of cleat in coal from Western North China. International Journal of Coal Geology, 2001, 47, 51-62. | 5.0 | 132 |
| 51 | Deformation Mechanisms and Macromolecular Structure Response of Anthracite under Different Stress. Energy & Fuels, 0, , . | 5.1 | 19 |